Journal of the European Ceramic Society xxx (2017) xxx–xxx

Contents lists available at www.sciencedirect.com

Journal of the European Ceramic Society

journal homepage: www.elsevier.com/locate/jeurceramsoc

Feature article

Developing titania-hydroxyapatite-reduced graphene oxide nanocomposite coatings by liquid flame spray deposition for photocatalytic applications

Jing Huang, Yongfeng Gong, Yi Liu, Xinkun Suo, Hua Li*

Key Laboratory of Marine Materials and Related Technologies, Zhejiang Key Laboratory of Marine Materials and Protective Technologies, Ningbo Institute of Materials Technology and Engineering, Chinese Academy of Sciences, Ningbo 315201, China

ARTICLE INFO

Article history:
Received 30 November 2016
Received in revised form 14 February 2017
Accepted 15 February 2017
Available online xxx

Keywords:
Titania
Hydroxyapatite
Reduced graphene oxide
Nanocomposite
Photocatalytic performance

ABSTRACT

Nanostructured titania has been extensively investigated for photocatalytic applications. Persistent challenge yet is how to effectively promote adhesion of microorganisms on the material surface for consequent enhanced photocatalytic disinfection. Here we report fabrication and characterization of titania-based nanocomposite coatings with addition of hydroxyapatite-reduced graphene oxide (HA-rGO). The nano features of TiO_2, HA, and rGO were well retained during liquid flame spray deposition. Photocatalytic activities of the coatings were examined by degradation of methylene blue and sterilization testing of *Escherichia coli* bacteria. Addition of HA-rGO effectively increased the specific surface area of the coatings and markedly enhanced adherence of the bacteria for subsequent extinguishment. The TiO_2–10 wt.% (HA-rGO) coating showed the best photocatalytic performances and further overloading of HA-rGO resulted in enwrapping of TiO_2 particles, resulting in deteriorated degradation activity. The results give clear insight into fabrication of novel photocatalytic nanocomposites by suspension thermal spray route for enhanced performances.

1. Introduction

Bacterium-related environmental issues like presence of microorganisms in drinking water have been gaining intensive concerns globally [1]. Pathogenic microorganisms, such as *Escherichia coli* (*E. coli*), *Virbio cholerae*, *Listeria monocytogens*, *Shigella* spp., and *Pseudomonas* spp., etc., in water resources lead to severe water-borne illness [2–4]. Various physical, chemical, and biological methods are therefore developed to remove microorganisms and/or pollutants [5]. To date, chlorination has been widely used for water treatment, including disinfection process for drinking water supplies and the tertiary treatment of wastewater effluents [6]. It is effective in inactivation of bacteria and most viruses [7]. However, the processing route is becoming of increasing concern due to the formation of potentially harmful chloro-organic disinfection by-products exerting carcinogenic and mutagenic influence on mammals [7,8]. Hence, new alternative disinfection techniques are urgently needed. Compared with conventional water treatment methods, such as UV irradiation, filtration and ozonization, photocatalysis showed great potential for inactivation of pathogenic microorganisms and has attracted much attention in recent years due to its advantages like nontoxicity, excellent degradation capability and cost efficiency [9–11].

Since the discovery of photo-induced splitting of water on titania electrodes by Fujishima and Honda [12], TiO_2 has been one of the key materials for photocatalytic applications and was widely used [9–11,13]. Inspired by the early work of Matsunaga et al. reported in 1985 [14], many research groups explored TiO_2-based photocatalysts and found successful killing of different microorganisms including bacteria, viruses, algae, fungi or protozoa [2,15]. Hydroxyl radical (•OH) generated by photocatalysis is found to oxidize and/or diffuse through cell wall/membrane, subsequently causing oxidation of intracellular coenzyme [16,17]. However, in most cases, TiO_2 can only decompose substances that come into contact, and it fails to work while there is no light [17,18]. Taking into account the prerequisite of intimate contact between bacteria and the antibacterial material, the material must essentially favor attachment of bacteria [17]. There are many techniques to improve the adsorption behavior and photocatalytic activities of TiO_2 [19]. Among them, heterogeneous photocatalysis system has been well established to improve the performances [20,21].

* Corresponding author.
E-mail address: lihua@nimte.ac.cn (H. Li).

http://dx.doi.org/10.1016/j.jeurceramsoc.2017.02.029
0955-2219/

Hydroxyapatite ($Ca_{10}(PO_4)_6(OH)_2$, HA), which has a similar chemical composition to the mineral component in natural bones and teeth, is of great interest in bone and tissue engineering. It has excellent biocompatibility, bioactivity and high affinity to proteins and lipids [22,23]. Use of HA or HA-based composites as additives in titania-based composites was therefore attempted to promote the recruitment of microorganisms or organics for subsequent photocatalytic degradation [17]. In addition, research efforts on HA/nano-carbon composites, such as HA-graphene composites, have been reported [24–26]. Progress has been made recently in fabrication of graphene-containing inorganic composites attributed to the promising properties of graphene, including unique electronic property, high transparency, flexible structure and large theoretical specific surface area [24,27,28]. Previous studies suggested that the incorporation of graphene could enhance the mechanical properties and bioactivity of HA-based composites [24–28]. Graphene-based nanomaterials could also inhibit the growth of *E. coli* while showing minimal cytotoxicity [29]. Moreover, like other carbon nanomaterials such as CNTs and fullerene, graphene-based materials have also been explored for potential photocatalytic applications [30]. It was reported that graphene could enhance the charge transfer of electrons and decrease the recombination of electron-hole pairs, which in turn improved the photocatalytic properties of TiO_2 [30,31].

For photocatalytic applications, several practical problems arise from the use of catalysts in powder form [21,30], such as difficulties in separating them from suspension or aggregation of particles in suspension [17]. Therefore, the form of coating/film is more appropriate for photocatalysts [32], which has been extensively investigated by using various processing techniques like sol-gel, chemical vapor deposition, electro-deposition, hydrothermal and thermal spray [17,33,34]. Liquid thermal spray uses liquid, for instance solution or suspension, as the starting feedstock and shows great promises in making functional coatings from nanoparticles [35–37]. Antimicrobial glassy coatings were successfully fabricated by high velocity suspension flame spray on titanium plates without degrading the substrate or forming chemical byproducts [36]. Liquid thermal spray processing route can effectively avoid possible phase transformation of sprayed materials and accomplishes favorable microstructural features such as desired porosity and high specific surface area, facilitating functional performances [17,37–39].

In this work, HA-rGO nanocomposite slurry was prepared by adding rGO sheets into the solution for synthesizing HA by the wet-chemical approach [24]. According to our previous findings that addition of 10 wt.% HA brought about the most significantly promoted photocatalytic performances of titania-based coatings [17], TiO_2–10 wt.%(HA-rGO) nanocomposite coatings were fabricated by liquid flame spray. Enhanced adherence of *E. coli* bacteria and adsorption of methylene-blue were revealed and elucidated, showing great potential of the coatings for photocatalytic applications.

2. Materials and methods

Commercial aluminum wire (Al, Ø2 mm, Beijing General Research Institute of Mining &Metallurgy, China), TiO_2 powder (pure anatase, 5 ~ 10 nm, Aladdin, Shanghai, China), hydroxyapatite (HA, lab-made needle-like particles of ~200 nm in length and 20–40 nm in diameter) and HA-reduced graphene oxide (HA-rGO) nanocomposite slurry (lab-made HA–10 wt.%rGO) were used. The HA or HA–10 wt.%rGO slurry was synthesized by a wet-chemical approach described in detail previously [24]. 316L stainless steel plates with the dimension of 20 × 20 × 2 mm in length, width and thickness, respectively, were used as the substrates. Prior to the deposition of the titania-based coatings, an aluminum coating with ~100 μm in thickness was pre-coated on the substrate to facilitate adhesion of the nanocomposite layer. The high velocity arc spray system (TLAS-500C, China) was employed to deposit the Al coatings. *Escherichia coli* bacteria (*E. coli*, ATCC 25922) were typically selected for bacterial adherence testing. Aqueous solution (5 ppm) of methylene blue (MB, Aladdin, Shanghai, China) was used as a model pollutant.

A series of suspensions (HA-rGO, TiO_2–10 wt.%(HA-rGO) and TiO_2–30 wt.%(HA-rGO)) were prepared by suspending 5 g of each sample in 150 ml deionized water and mixing in an ultrasonic disintegrator for 10 min before the spraying. The coatings were then fabricated by liquid flame spray (DS 8000, Eutectic Castolin, Germany). A suspension injector with the diameter of 1.5 mm was positioned just next to the flame torch, and the angle between the injector and flame was 30°. The pressure of the atomizing air was 0.7 MPa and the suspension feeding rate was 40 ml/min. Pressure of oxygen and acetylene was 0.5 MPa and 0.1 MPa, respectively. The flow rate of acetylene was 0.8 m^3/h and the spray distance was 200 mm.

Phases of the samples were detected by X-ray diffraction (XRD, Bruker AXS, Germany) with a scanning rate of 0.1°/s using monochromatic Cu-Ka radiation operated at 40 kV and 40 mA. Microstructural features of the powder and coatings were examined using field emission scanning electron microscope (FESEM, FEI Quanta FEG250, the Netherlands). Specific surface area of the coatings was measured using the Brunauer, Emmett, and Teller (BET) method by adsorption of nitrogen gas on ASAP 2020 M apparatus at 77.3 K. The BET surface area was calculated over the relative pressure range of 0.05–0.20 MPa. For comparison purpose, pure HA, pure TiO_2 (TO) and TiO_2 with 10 wt.%HA (TiO_2–10 wt.%HA, TO10H) coatings were also investigated in this study.

Luria broth (LB, Aladdin, Shanghai, China) medium used in this study comprised 10 g tryptone, 10 g sodium chloride, and 5 g yeast extract in 1 l deionized water. After inoculation of a single colony of *E. coli*, the media were shaken at 150 rpm for 24 h at 30 °C. Bacteria were then harvested by centrifugation at 2000 rpm for 5 min. After removal of the supernatant, bacteria were washed with phosphate-buffered saline (PBS) and resuspended in PBS at a concentration of 5×10^6 CFU/ml. The coating samples were put into a 12-well plate and then 2 ml of the bacterial suspension was added to each well. The plate was incubated at 30 °C for 6 h in dark for bacterial adhesion. For SEM observation, the samples were first rinsed with PBS to remove non-adherent bacteria. Then the samples were fixed in 2.5% glutaraldehyde at 4 °C overnight and rinsed twice in PBS. Further dehydration and critical-point drying steps were conducted using a graded series of ethanol/water solutions as described in another paper [17]. Enumeration of attached cells was carried out by counting the cells from the SEM images. Digital images were taken randomly from at least five locations for each sample.

Photocatalytic degradation activity of the coatings was evaluated by degradation of MB aqueous solution. Each sample was put into to a Ø9 cm Petri dish with 20 ml MB solution (5 ppm) followed by UV-irradiation. The irradiation was conducted using a 15 W UV lamp (PHILIPS, TLD15W BL) with the typical wave length of 365 nm, and the distance between the UV light source and the samples was 150 mm. Variation of MB concentration as determined by the absorbance at 664 nm was analyzed using a spectrophotometer (SpectraMax 190, Molecular Devices, USA).

Photocatalytic sterilization activity of the coating samples under UV-illumination was assessed using a similar suspension method reported previously [17]. The nutrient agar culture medium (Huankai Microbial Sci. Tech. Co. Ltd., China) used in this study comprised 33 g nutrient agar cultured in 1 l deionized water, and was autoclaved at 120 °C for 15 min. Then 15 ml of the nutrient agar media were poured into each Ø9 cm Petri dish. After UV-irradiation

Please cite this article in press as: J. Huang, et al., Developing titania-hydroxyapatite-reduced graphene oxide nanocomposite coatings by liquid flame spray deposition for photocatalytic applications, *J Eur Ceram Soc* (2017), http://dx.doi.org/10.1016/j.jeurceramsoc.2017.02.029

for a period of time, 100 μl of the *E. coli* bacterial suspension was spread in the agar media and incubated at 37 °C for 24 h. The bacteria number was determined by a standard plate count approach in triplicates. The colony-forming units (CFUs) of the bacteria were examined and bacterial survival ratios were calculated according to the equation:

$$\text{Bacterial survival ratio} = \frac{\text{CFUs of blank group - CFUs of experimental group}}{\text{CFUs of blank group}} \times 100\%.$$

The blank group was prepared by incubating the substrate samples in 4 ml bacterial suspension.

3. Results and discussion

3.1. Characteristics of the coatings

XRD spectra of the TiO_2/HA/rGO nanocomposite coatings show that the anatase structure of TiO_2 is well retained, and no rutile structure is detected (Fig. 1a). These results suggest that there is little or no phase transformation of nano-TiO_2 from anatase to rutile during the spraying. The broad XRD peak of HA is seen at ~31° of 2θ, indicating low crystallinity of HA synthesized by the wet chemical precipitation method and presumable presence of HA grains in small size [40]. During the liquid flame spray, evaporation of liquid takes away plenty of heat and greatly reduces the heating temperature of nano-TiO_2, which would in turn effectively avoid overheating and phase transformation [35,38]. It was reported variations in heating extent of the nanoparticles were attained by altering suspension plasma spray parameters or suspension feeding mode [37]. Moreover, HA is a low thermal conductivity material as compared to TiO_2, giving rise to weakened heat conduction for inhibited phase changes of titania [41]. XRD diffraction peaks for rGO are not observed, most likely due to the fact that the monolayer structure of rGO exhibits irregular arrays of atoms in three dimensions [24]. Instead, refined detection by Raman spectroscopy confirms the presence of rGO in the composite coatings (Fig. 1b). The characteristic peaks of rGO are successfully detected in the HG and the TO30HG samples but not in the TO10HG sample, which might be due to the low content of rGO. The first-order spectrum of graphene is suggested by the *G* band at 1583 cm^{-1} and the *D* band at 1329 cm^{-1}, respectively. The second-order (two-photon) spectra at 2647 cm^{-1} refer to 2*D* band of graphene in the coatings [26]. It is well known that Raman spectrum can be used to assess the quality of graphene and determine the number of graphene sheets by the position of 2D peak [42]. The shift of 2D peak to lower wavenumber values likely suggests that there is less layer of rGO in the coating (spectrum (HG) in Fig. 1b) and the features of rGO are well retained.

Topographical morphology of the coatings was examined by SEM (Fig. 2). Remarkably different topographical structures of the HA-based coatings and the Ti-based coatings are seen (Fig. 2a, b versus c-f). The HA-based coatings are in sheet shape with no sign of melting after deposition. HA underwent nucleation growth on rGO layers and retained their original needle-like shape (Fig. 2b and enlarged view of selected area shown in Fig. 2g). However, titania nanoparticles mostly aggregate and form spherical-like micron particles with a diameter of 1–2 μm and their surfaces show clear signs of melting (Fig. 2f). For the TiO_2-based composite coatings, HA-rGO additives disperse in the coatings and are mechanically interlocked among TiO_2. In addition, individual or small groups of HA-rGO sheets adhere to micron-sized titania particles or disperse among them, which would be conductive to enhance the photocatalytic function of titania. Moreover, typical cross-sectional view of the coatings suggest the thickness of 120–150 μm for the double layers and 20–30 μm for the nanocomposite coatings (Fig. 2h).

3.2. Adherence behaviors of E. coli bacteria on the coatings

After being incubated in bacteria solution (5×10^6 CFU/ml) for 6 h, *E. coli* bacteria already attached on the coating surfaces. In this study, *E. coli* was allowed to interact with the coatings for a relatively long duration. That more bacteria attached on the coating surfaces means better capability of the coatings to recruit the bacteria. SEM images clearly show that the number of the bacteria adhered on the surface of the pure TiO_2 (TO) coating is much less than the number of the bacteria attached on the pure HA, the pure HA-rGO and the TiO_2-based composite coatings (Fig. 3a). The number of the bacteria adhered on the coating surfaces was counted from the SEM images, which is a well-established approach [43], as shown in Fig. 3b. The HA-rGO nanocomposites show better bioactivity than the pure HA, and this is consistent with our previous findings [17,26,44]. It was reported that graphene or reduced graphene oxide in HA-based composites stimulated cellular pseudopod attachment and enhanced the viability of cells [26,29]. The bioactivity of TiO_2-based coatings is significantly enhanced by the addition of the biomaterials, HA or HA-rGO in this case. It is consistently observed that increase in HA-rGO content is accompanied with promoted adherence of the bacteria. *E. coli* preferably adhere to the composite coatings, and the number of the adherent bacteria on the TO30HG coating is almost eight times more than that adhered on the pure TiO_2 coating (Fig. 3b). Bacterial preference to the additives is also evidenced by the selective adherence of the bacteria on HA or HA-rGO sheets in the composite coatings, rather than on micron-sized TiO_2 particles. This is clearly observed from the topographical views of the TO10HG or TO30HG coatings (Fig. 3a). A two-phase process usually occurs during bacterial adhesion onto material, namely phase one (physicochemical interactions) and phase two (molecular and cellular interactions) [45]. For phase two, molecular reactions between bacterial surfaces and material surfaces are predominant. Polysaccharides and proteins on the surfaces of cells/bacteria act as their adhesions [45–47]. Bioactive materials such as HA-based materials have high affinity to proteins and lipids, therefore their addition into TiO_2 coatings would certainly promote bacterial adhesion. As mentioned above, HA-rGO nanocomposite sheets are thoroughly dispersed in the coatings and are mechanically interlocked among TiO_2 (Fig. 2f). The bacteria attached on HA-rGO are also in contact with TiO_2. Thus, bioactive materials in the coatings likely act as baits which attract bacteria and push them to titania. Once the photocatalytic reactions take place, extinguishment of the bacteria is anticipated. Incorporation of HA-rGO into titania is therefore expected to possess a better antibacterial performance in terms of efficiency, especially when much more bacteria are dispersed in surrounding media.

3.3. Photocatalytic performances of the coatings

Photocatalytic performances of the coatings were assessed by photodegradation of the MB-containing solution and photocatalytic disinfection of *E. coli* bacteria under UV irradiation. For photodegradation of MB, before UV irradiation, the MB-containing solution was completely mixed with the samples in dark for 1 h to ensure adsorption/desorption equilibrium. It is clear that the degradation is enhanced by elongated UV exposure and the decomposition rate decreases with the increase in reaction time (Fig. 4a). Addition of HA or HA-rGO nanocomposites significantly improves the photocatalytic degradation of TiO_2-based coatings. The coating containing 10 wt.%HA-rGO (TO10HG) shows excellent photodegradation performance with ~78% degradation of MB after 5.5 h exposure. On the contrary, the pure TiO_2 coating shows much worse photocatalytic performance with ~35% degradation of MB. The addition of 10 wt.%HA-rGO showed the best photodegradation activity, which is consistent with our previous work [17]. The

Please cite this article in press as: J. Huang, et al., Developing titania-hydroxyapatite-reduced graphene oxide nanocomposite coatings by liquid flame spray deposition for photocatalytic applications, *J Eur Ceram Soc* (2017), http://dx.doi.org/10.1016/j.jeurceramsoc.2017.02.029

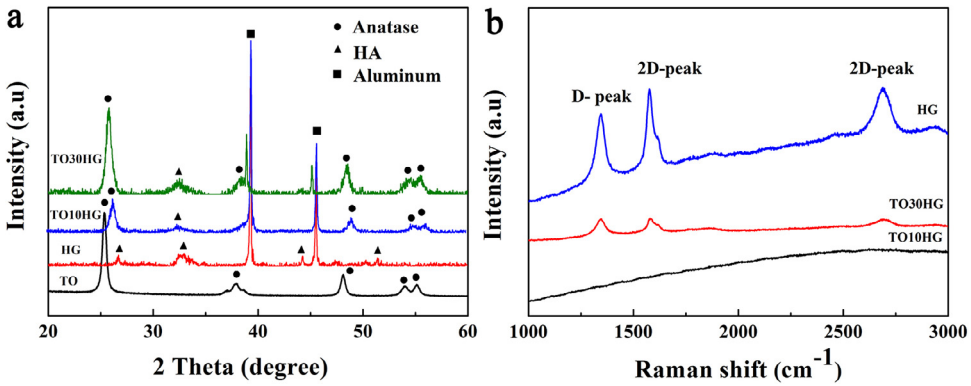

Fig 1. XRD curves (a) and Raman spectra (b) of the coatings. TO: the pure titania coating, HG: the HA-rGO coating, TO10HG: the TiO_2–10 wt.% (HA-rGO) coating, TO30HG: the TiO_2–30 wt.% (HA- rGO) coating.

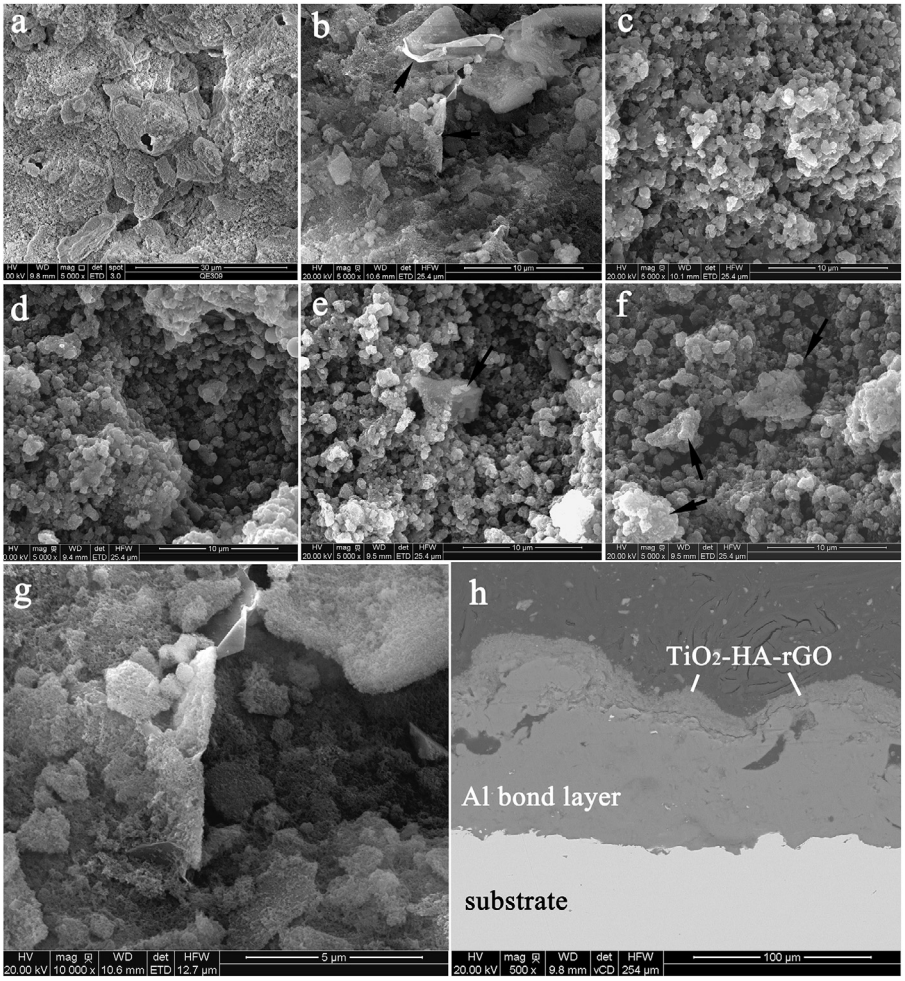

Fig. 2. Surface views of the as-deposited nanostructured coatings, (a) the pure HA coating, (b) the HA-rGO coating, (c) the pure TiO_2 coating, (d) the TiO_2–10 wt.%HA coating, (e) the TiO_2–10 wt.%(HA-rGO) coating, (f) the TiO_2–30 wt.%(HA-rGO) coating, (g) enlarged view of selected area shown in (b) showing nucleation and further growth of HA on rGO layer, and (h) cross-sectional view of the TiO_2–30 wt.%(HA-rGO) coating. The black arrows point to typical HA-rGO existing in the coatings.

TO10HG coating has better degradation efficiency than the TO30HG and the TO10H coatings. It was previously reported that photocatalytic materials must adsorb and contact with pollutants to degrade them [18]. As typical biomedical materials, HA and rGO have excellent adsorption properties [25,31]. Specific surface area is one of the important indexes for catalysts and adsorbents and higher specific surface area usually provides catalysts with better photocatalytic activity and adsorptive properties for inorganics, organics, and microorganisms [16]. Specific surface areas of the coatings were therefore measured to elucidate their performances. The composite coatings containing HA or HA-rGO composites obviously exhibit higher specific surface areas than the pure titania coatings. The TO10H, TO10HG and TO30HG have the specific surface area values of 0.47 m^2/g, 0.53 m^2/g, and 0.83 m^2/g, respectively (Fig. 4b), while the pure titania coating shows the value of 0.46 m^2/g. This is presumably due to the high specific surface area of HA or HA-rGO. For

Please cite this article in press as: J. Huang, et al., Developing titania-hydroxyapatite-reduced graphene oxide nanocomposite coatings by liquid flame spray deposition for photocatalytic applications, *J Eur Ceram Soc* (2017), http://dx.doi.org/10.1016/j.jeurceramsoc.2017.02.029

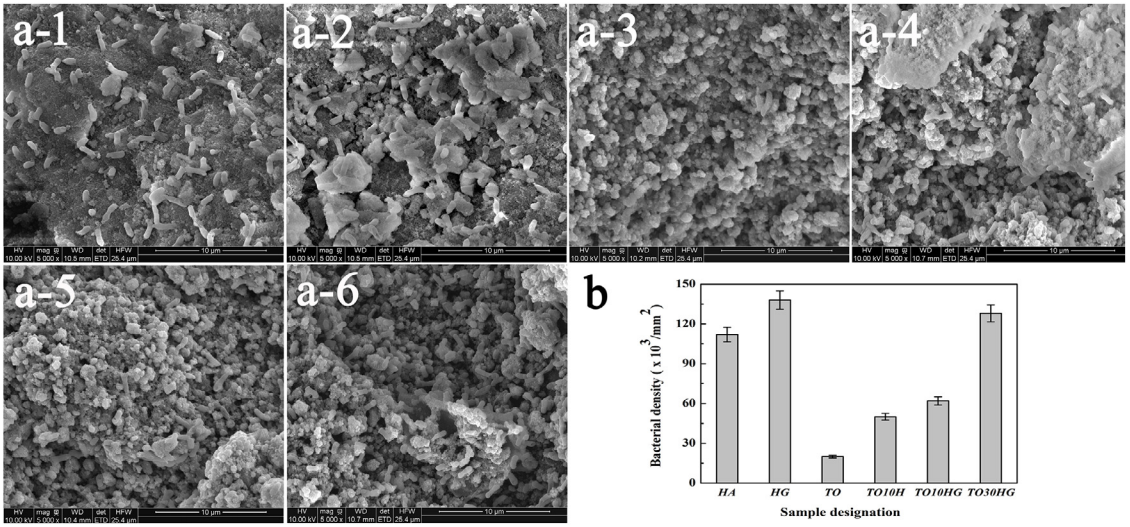

Fig. 3. (a) SEM images of *E. coli* adhered on the coatings after incubation for 6 h: –1 the pure HA coating, –2: the HA-rGO coating, –3: the pure titania coating, –4: the TiO_2–10 wt.%HA coating, –5: the TiO_2–10 wt.%(HA-rGO) coating, –6: the TiO_2–30 wt.%(HA-rGO) coating, and (b) bacterial density as determined by statistical counting of the *E. coli* adhered on the surfaces of the coatings. Digital images were taken randomly from at least five locations for each sample, and the number of the bacteria in each image was counted for averaged value.

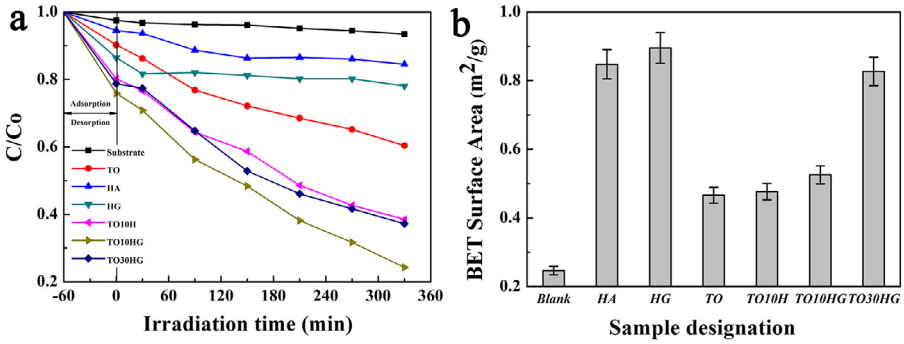

Fig. 4. Degradation efficiency of MB by the coatings under UV illumination (a), and specific surface area values of the coatings as measured by the N_2-BET approach (b).

the TiO_2-based nanocomposite coatings, their MB degradation tendency agrees well with their specific surface area data (TO10H and TO10HG). Surprisingly, the TO10HG coating shows better degradation than the TO30HG coating, which has higher specific surface area. This might be due to the addition of too much HA-rGO, since HA-rGO has less photocatalytic activity than titania. Overloading of HA-rGO might shield the TiO_2 particles such that the particles fail to function entirely for photocatalytic functions. The higher specific surface area exhibited by the pure HA or the HG coatings is mainly due to the small-sized HA grains and the intrinsic properties of graphene [17,30]. HA or HG existing in the coatings are in sheet shape and the nanostructures are fully exposed, providing enlarged contact area for photocatalytic reactions (Fig. 2b). Although TiO_2 particles are also very small (5–10 nm), they could easily get aggregated to form micron-sized particles (1–2 μm) after the spraying. Furthermore, since their surfaces are partially melted, this could further reduce their specific surface area (Fig. 2f). Obviously, appropriate addition of HA-rGO could attain the synergistic effect, giving rise to significantly enhanced photocatalytic performances.

Further photocatalytic testing against *E. coli* shows that the TiO_2-based nanocomposite coatings possesses excellent photocatalytic sterilization performances. Digital photos of *E. coli* colonies in Petri dish and statistical results of the samples after 1 h UV irradiation are shown in Fig. 5. The blank sample and the pure HG coating exhibit undetectable photocatalytic sterilization (Fig. 5a). In contrast, the number of the colonies in the Petri dishes containing the TO10H, the TO10HG, and the TO30HG coating samples is significantly less than that of the pure TiO_2, implying their outstanding photocatalytic sterilization properties. To further assess the bacteria-killing capability of the coating samples, bacterial survival ratio was calculated (Fig. 5b). After 1 h UV irradiation, more than 90% bacteria are killed by the TO10H and the TO10HG coatings. However, the nanocomposite coatings containing less HA or HA-rGO have better photocatalytic performances, which is consistent with the trend of MB degradation (Fig. 4a). The nanocomposite coatings with the addition of 10 wt.% HA-rGO exhibit the most significant enhancement of disinfection, ~95%. On the contrary, only 87.3% of *E. coli* removal is obtained in 60 min when HA-rGO loading is further increased to 30 wt.%. More HA-rGO addition means more graphene loading, which would increase the opacity and light scattering and hinder TiO_2 from adsorbing light, resulting in deteriorated photocatalytic activity [48,49]. Moreover, too much HA-rGO loading would cover the surface of nano-TiO_2 aggregates, which have the size of 1–2 μm (Fig. 2f). Owing to the similar size of *E. coli* cells (~1 μm in diameter and ~2 μm in length) [50], access of bacteria to the internal surfaces of nano-TiO_2 materials might be impeded [13]. The redundant HA-rGO composites reduce both access to *E. coli* and relative availability of active sites. As a consequence, *E. coli* inactivation would be weakened.

Photocatalytic mechanism of nano titania has been extensively studied. Photocatalytic reaction of TiO_2 proceeds via the generation of electrons and holes from irradiation with UV light. As

Please cite this article in press as: J. Huang, et al., Developing titania-hydroxyapatite-reduced graphene oxide nanocomposite coatings by liquid flame spray deposition for photocatalytic applications, *J Eur Ceram Soc* (2017), http://dx.doi.org/10.1016/j.jeurceramsoc.2017.02.029

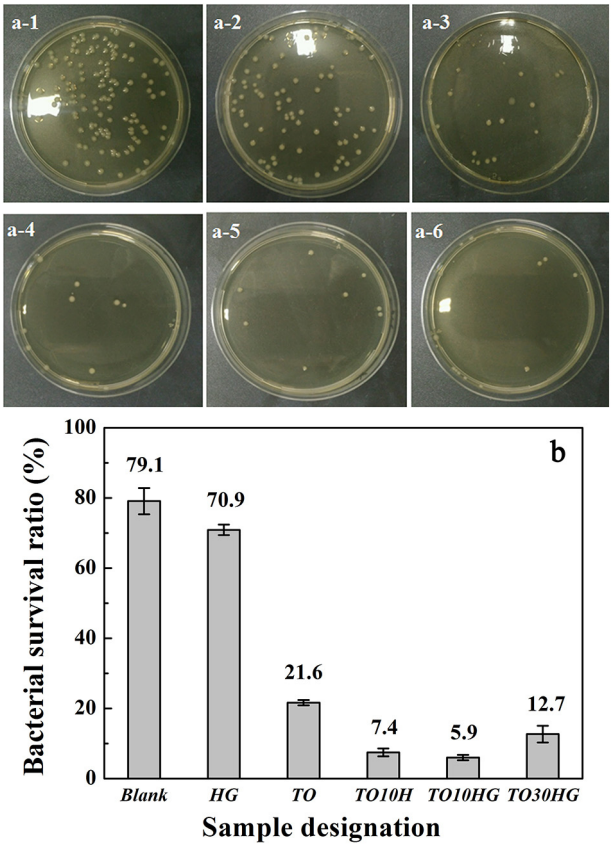

Fig. 5. Photocatalytic sterilization results of the coatings against *E. coli*. (a) digital photos of *E. coli* colonies in the petri dish containing all samples after 1 h UV irradiation: −1: the pure HA coating, −2: the HA-rGO coating, −3: the pure titania coating, −4: the TiO_2–10 wt.%HA coating, −5: the TiO_2–10 wt.%(HA-rGO) coating, −6: the TiO_2–30 wt.%(HA-rGO) coating, and (b) antibacterial performances of the coatings against *E. coli*.

the consequence, •OH is generated by the reaction of holes in the valence bands with active OH^- on the surface or with H_2O [51,52]. The conduction band electron reduces oxygen to $•O_2^-$, and further reduction of $•O_2^-$ produces H_2O_2. The superoxide can react with H_2O_2 to produce •OH. Oxygen radicals attack bacterial organic components, including outer membrane, DNA, RNA, and lipid, to oxidize or damage them, ultimately causing bacterial death [3,51,52]. *E. coli*, as a Gram-negative bacterium, has a large number of polyunsaturated phospholipids as integral components of cell membrane [53,54]. Oxygen radicals oxidize the polyunsaturated phospholipid components in cell membrane and further generate pores, causing destruction of cell membranes followed by shape change from rod-like to flattened [55]. Loss of intact membrane structure and hence the functions is the fundamental cause of cell death [3,56]. Compared with the TO10H sample, the TO10HG coating exhibited slight enhancement of photocatalytic sterilization ability. In this study, coupling TiO_2 with rGO did not enhance the disinfection efficiency of TiO_2 nanoparticles and the main reason of better photocatalytic properties lies in the addition of HA. The impact of addition of rGO on the performances of the coatings, such as electronic transmission, conductivity and adsorptivity [57], yet needs to be further studied. rGO improves the bioactivity, absorptivity and specific surface area of the HA-based composites, which would ultimately affect the performances of the TiO_2/HA/rGO composite coatings.

For photocatalytic applications, the key issues pertain to the questions as to how to use catalysts as film or coating [17,32], and how to use efficiently the visible light [31]. In practical systems using light sources such as white light fluorescent lamps and solar light, which have very weak UV radiation intensities, the photocatalyst exhibits weak disinfection activity [30,31]. Previous studies showed that addition of rGO to photocatalytic materials could effectively improve the utilization rate of visible light [31]. Our ongoing efforts are therefore devoted to developing TiO_2/HA/rGO photocatalytic materials and their coatings that can be activated by visible light. The role rGO played in the photocatalytic coatings is yet to be further elucidated.

4. Conclusions

Nanostructured titania coatings with addition of HA-rGO nanocomposites (10, 30 wt.%) have been successfully fabricated by suspension flame spraying. The structural features of TiO_2 and HA-rGO nanocomposites are well retained during the deposition. Addition of HA-rGO effectively increases the specific surface area of the titania-based coatings and markedly enhances the adherence of *E. coli* bacteria for subsequent photocatalytic killing. The coating fabrication by the suspension flame spray route of the novel TiO_2-HA-rGO materials might open a new window for making photocatalytic layers for enhanced performances.

Acknowledgements

This research was supported by National Natural Science Foundation of China (grant # 31271017 and 41476064), Key Research and Development Program of Zhejiang Province (grant # 2017C01003), and Ningbo Major R&D Project (grant # 2015B11054).

References

[1] R. Fayer, Cryptosporidium: a water-borne zoonotic parasite, Vet. Parasitol. 126 (2004) 37–56.
[2] O.K. Dalrymple, E. Stefanakos, M.A. Trotz, D.Y. Goswami, A review of the mechanisms and modeling of photocatalytic disinfection, Appl. Catal. B: Environ. 98 (2010) 27–38.
[3] S. Swetha, S.M. Santhosh, R.G. Balakrishna, Synthesis and comparative study of nano-TiO_2 over Degussa P-25 in disinfection of water, Photochem. Photobiol. 86 (2010) 628–632.
[4] J.R. Steter, W.R.P. Barros, M.R.V. Lanza, A.J. Motheo, Electrochemical and sonoelectro-chemical processes applied to amaranth dye degradation, Chemosphere 117 (2014) 200–207.
[5] J. Vijayaraghavan, S.J. Sardhar Basha, J. Jegan, A review on efficacious methods to decolorize reactive azo dye, J. Urb. Environ. Eng. 7 (2013) 30–47.
[6] J. Darby, M. Heath, J. Jacangelo, F. Loge, P. Swaim, G. Tchobanoglous, Comparison of UV Irradiation to Chlorination: Guidance for Achieving Optimal UV Performance, Project 91-WWD-1, Water Environment Research Foundation (WERF), Alexandria, VA USA, 1995.
[7] S.D. Richardson, Disinfection by-products and other emerging contaminants in drinking water, Trac Trend. Anal. Chem. 22 (2003) 666–684.
[8] C. Pablos, R. van Grieken, J. Marugan, I. Chowdhury, S.L. Walker, Study of bacterial adhesion onto immobilized TiO_2: Effect on the photocatalytic activity for disinfection applications, Catal. Today 209 (2013) 140–146.
[9] M.N. Chong, B. Jin, C.W.K. Chow, C. Saint, Recent developments in photocatalytic water treatment technology: a review, Water Res. 44 (2010) 2997–3027.
[10] S. Malato, P. Fernandez-Ibanez, M.I. Maldonado, J. Blanco, W. Gernjak, Decontamination and disinfection of water by solar photocatalysis: recent overview and trends, Catal. Today 147 (2009) 1–59.
[11] D. Spasiano, R. Marotta, S. Malato, P. Fernandez-Ibanez, I. Di Somma, Solar photocatalysis: materials, reactors, some commercial, and pre-industrialized applications. A comprehensive approach, Appl. Catal. B: Environ. 170 (2015) 90–123.
[12] A. Fujishima, K. Honda, Electrochemical photolysis of water at a semiconductor electrode, Nature 238 (1972) 37–38.
[13] G. Wang, W. Feng, X. Zeng, Z. Wang, C. Feng, D.T. McCarthy, A. Deletic, X. Zhang, Highly recoverable TiO_2-GO nanocomposites for stormwater disinfection, Water Res. 94 (2016) 363–370.
[14] T. Matsunaga, R. Tomoda, T. Nakajima, H. Wake, Photoelectrochemical sterilization of microbial cells by semiconductor powders, Fems Microbiol. Lett. 29 (1985) 211–214.
[15] O. Ruzimuradov, S. Nurmanov, M. Hojamberdiev, R.M. Prasad, A. Gurlo, J. Broetz, K. Nakanishi, R. Riedel, Fabrication of nitrogen-doped TiO_2 monolith with well-defined macroporous and bicrystalline framework and its

photocatalytic performance under visible light, J. Eur. Ceram. Soc. 34 (2014) 809–816.
[16] R.P.S. Suria, H.M. Thorntonb, M. Muruganandhama, Disinfection of water using Pt- and Ag-doped TiO_2 photocatalysts, Environ. Technol. 33 (2012) 1651–1659.
[17] Y.X. Liu, J. Huang, S.Y. Ding, Y. Liu, J.H. Yuan, H. Li, Deposition characterization, and enhanced adherence of *Escherichia coli* bacteria on flame-sprayed photocatalytic titania-hydroxyapatite coatings, J. Therm. Spray Technol. 2 (2013) 1053–1062.
[18] T. Nonami, H. Hase, K. Funakoshi, Apatite-coated titanium dioxide photocatalyst for air purification, Catal. Today 96 (2004) 113–118.
[19] J.B. Cai, X.Q. Wu, S.X. Li, F.Y. Zheng, Controllable location of Au nanoparticles as cocatalyst onto TiO_2@CeO_2 nanocomposite hollow spheres for enhancing photocatalytic activity, Appl. Catal. B: Environ. 201 (2017) 12–21.
[20] V. Augugliaro, M. Litter, L. Palmisano, J. Soria, The combination of heterogeneous photocatalysis with chemical and physical operations: a tool for improving the photoprocess performance, J. Photochem. Photobiol. C 7 (2006) 127–144.
[21] W.C. Lin, C.N. Chen, T.T. Tseng, M.H. Wei, J.H. Hsieh, W.J. Tseng, Micellar layer-by-layer synthesis of TiO_2/Ag hybrid particles for bactericidal and photocatalytic activities, J. Eur. Ceram. Soc. 30 (2010) 2849–2857.
[22] S. Zeng, S.Z. Fu, G. Guo, H. Liang, Z.Y. Qian, X.H. Tang, F. Luo, Preparation and characterization of nano-hydroxyapatite/poly(vinyl alcohol) composite membranes for guided bone regeneration, J. Biomed. Nanotechnol. 7 (2011) 549–557.
[23] K. Ozeki, J.M. Janurudin, H. Aoki, Y. Fukui, Photocatalytic hydroxyapatite/titanium dioxide multilayer thin film deposited onto glass using an rf magnetron sputtering technique, Appl. Surf. Sci. 253 (2007) 3397–3401.
[24] Y. Liu, J. Huang, H. Li, Synthesis of hydroxyapatite-reduced graphite oxide nanocomposites for biomedical applications: oriented nucleation and epitaxial growth of hydroxyapatite, J. Mater. Chem. B 1 (2013) 1826–1834.
[25] A. Jankovic, S. Erakovic, M. Mitric, I.Z. Matic, Z.D. Juranic, G.C.P. Tsui, C.Y. Tang, V. Miskovic-Stankovic, K.Y. Rhee, S.J. Park, Bioactive hydroxyapatite/graphene composite coating and its corrosion stability in simulated body fluid, J. Alloy Compd. 624 (2015) 148–157.
[26] Y. Liu, Z. Dang, Y. Wang, J. Huang, H. Li, Hydroxyapatite/graphene-nanosheet composite coatings deposited by vacuum cold spraying for biomedical applications: inherited nanostructures and enhanced properties, Carbon 67 (2014) 250–259.
[27] G.M. Neelgund, A. Oki, Z. Luo, In situ deposition of hydroxyapatite on graphene nanosheets, Mater. Res. Bull. 48 (2013) 175–179.
[28] L. Zhang, W. Liu, C. Yue, T. Zhang, P. Li, Z. Xing, Y. Chen, A tough graphene nanosheet/hydroxyapatite composite with improved in vitro biocompatibility, Carbon 61 (2013) 105–115.
[29] T.R. Nayak, H. Andersen, V.S. Makam, C. Khaw, S. Bae, X.F. Xu, P.L.R. Ee, J.H. Ahn, B.H. Hong, G. Pastorin, B. Ozyilmaz, Graphene for controlled and accelerated osteogenic differentiation of human mesenchymal stem cells, Acs Nano 5 (2011) 4670–4678.
[30] H. Zhang, X.J. Lv, Y.M. Li, Y. Wang, J.H. Li, P25-graphene composite as a high performance photocatalyst, Acs Nano 4 (2010) 380–386.
[31] T.W. Kim, M. Park, H.Y. Kim, S.J. Park, Preparation of flower-like TiO_2 sphere/reduced graphene oxide composites for photocatalytic degradation of organic pollutants, J. Solid State Chem. 239 (2016) 91–98.
[32] M. Uzunova-Bujnova, R. Todorovska, M. Milanova, R. Kralchevska, D. Todorovsky, On the spray-drying deposition of TiO_2 photocatalytic films, Appl. Surf. Sci. 256 (2009) 830–837.
[33] M. Kubo, H. Fukuda, X.J. Chua, T. Yonemoto, Kinetics of ultrasonic degradation of phenol in the presence of composite particles of titanium dioxide and activated carbon, Ind. Eng. Chem. Res. 46 (2007) 699–704.
[34] M.G. Nolan, M.E. Pemble, D.W. Sheel, H.M. Yates, One step process for chemical vapour deposition of titanium dioxide thin films incorporating controlled structure nanoparticles, Thin Solid Films 515 (2006) 1956–1962.
[35] P. Fauchais, G. Montavon, Latest developments in suspension and liquid precursor thermal spraying, J. Therm. Spray Technol. 19 (2009) 226–239.
[36] L.A. Díaz, B. Cabal, C. Prado, J.S. Moya, R. Torrecillas, A. Fernández, I. Arhire, P. Krieg, A. Killinger, R. Gadow, High-velocity suspension flame sprayed (HVSFS) soda-lime glass coating on titanium substrate: its bactericidal behaviour, J. Eur. Ceram. Soc. 36 (2016) 2653–2658.
[37] S. Kozerski, F.-L. Toma, L. Pawlowski, B. Leupolt, L. Latka, L.-M. Berger, Suspension plasma sprayed TiO_2 coatings using different injectors and their photocatalytic properties, Surf. Coat. Technol. 205 (2010) 980–986.
[38] F.L. Toma, L.M. Berger, D. Jacquet, D. Wicky, I. Villaluenga, Y.R. de Miguel, J.S. Lindelov, Comparative study on the photocatalytic behaviour of titanium oxide thermal sprayed coatings from powders and suspensions, Surf. Coat. Technol. 203 (2009) 2150–2156.
[39] Q.F. Wu, J. Huang, H. Li, Deposition of porous nano-WO_3 coatings with tunable grain shapes by liquid plasma spraying for gas-sensing applications, Mater. Lett. 141 (2015) 100–103.
[40] X.D. Wu, X.F. Song, D.S. Li, J.G. Liu, P.B. Zhang, X.S. Chen, Preparation of mesoporous nano-hydroxyapatite using a surfactant template method for protein delivery, J. Bionic. Eng. 9 (2012) 224–233.
[41] F.X. Ye, A. Ohmori, T. Tsumura, K. Nakata, C.J. Li, Microstructural analysis and photocatalytic activity of plasma-sprayed titania-hydroxyapatite coatings, J. Therm. Spray Technol. 16 (2007) 776–782.
[42] Y.W. Zhu, S. Murali, W.W. Cai, X.S. Li, J.W. Suk, J.R. Potts, R.S. Ruoff, Graphene and graphene oxide: synthesis, properties, and applications, Adv. Mater. 22 (2010) 5226.
[43] J. Tsibouklis, M. Stone, A.A. Thorpe, P. Graham, T.G. Nevell, R.J. Ewen, Inhibiting bacterial adhesion onto surfaces: the non-stick coating approach, Int. J. Adhes. Adhes. 20 (2000) 91–96.
[44] Y. Liu, J. Huang, H. Li, Nanostructural characteristics of vacuum cold-sprayed hydroxyapatite/graphene-nanosheet coatings for biomedical applications, J. Therm. Spray Technol. 23 (2014) 1149–1156.
[45] Y.H. An, R.J. Friedman, Concise review of mechanisms of bacterial adhesion to biomaterial surfaces, J. Biomed. Mater. Res. B 43 (1998) 338–348.
[46] K.D. Kroncke, I. Orskov, F. Orskov, B. Jann, K. Jann, Electron-microscopic study of coexpression of adhesive protein capsules and polysaccharide capsules in *Escherichia coli*, Infect. Immun. 58 (1990) 2710–2714.
[47] M. Fletcher, G.D. Floodgate, Electron-microscopic demonstration of an acidic polysaccharide involved in the adhesion of a marine bacterium to solid surfaces, J. Gen. Microbiol. 74 (1973) 325–334.
[48] P. Gao, D.D. Sun, Ultrasonic preparation of hierarchical graphene-oxide/TiO_2 composite microspheres for efficient photocatalytic hydrogen production, Chem. Asian. J. 8 (2013) 2779–2786.
[49] T. Szabo, A. Veres, E. Cho, J. Khim, N. Varga, I. Dekany, Photocatalyst separation from aqueous dispersion using graphene oxide/TiO_2 nanocomposites, Colloids Surf. A 433 (2013) 230–239.
[50] B. Volkmer, M. Heinemann, Condition-dependent cell volume and concentration of *Escherichia coli* to facilitate data conversion for systems biology modeling, PLoS One 6 (2011) e23126.
[51] M. Cho, H. Chung, W. Choi, J. Yoon, Linear correlation between inactivation of *E-coli* and OH radical concentration in TiO_2 photocatalytic disinfection, Water Res. 38 (2004) 1069–1077.
[52] H. Belhadj, A. Hakki, P.K.J. Robertson, D.W. Bahnemann, In situ ATR-FTIR study of H_2O and D_2O adsorption on TiO_2 under UV irradiation, Phys. Chem. Chem. Phys. 17 (2015) 22940–22946.
[53] K. Sunada, Y. Kikuchi, K. Hashimoto, A. Fujishima, Bactericidal and detoxification effects of TiO_2 thin film photocatalysts, Environ. Sci. Technol. 32 (1998) 726–728.
[54] E. Mileykovskaya, Subcellular localization of *Escherichia coli* osmosensory transporter prop: focus on cardiolipin membrane domains, Mol. Microbiol. 64 (2007) 1419–1422.
[55] J.W. Liou, M.H. Gu, Y.K. Chen, W.Y. Chen, Y.C. Chen, Y.H. Tseng, Y.J. Huang, H.H. Chang, Visible light responsive photocatalyst induces progressive and apical-terminus preferential damages on Escherichia coli surfaces, PLoS One 6 (2011) e19982.
[56] A. Villarino, M.N. Rager, P.A.D. Grimont, O.M.M. Bouvet, Are UV-induced nonculturable Escherichia coli K-12 cells alive or dead? Eur. J. Biochem. 270 (2003) 2689–2695.
[57] V. Stengl, D. Popelkova, P. Vlacil, TiO_2-graphene nanocomposite as high performace photocatalysts, J. Phys. Chem. C 115 (2011) 25209–25218.

Please cite this article in press as: J. Huang, et al., Developing titania-hydroxyapatite-reduced graphene oxide nanocomposite coatings by liquid flame spray deposition for photocatalytic applications, *J Eur Ceram Soc* (2017), http://dx.doi.org/10.1016/j.jeurceramsoc.2017.02.029